Imaging of the *In Situ* Deposition of Lead on Highly Oriented Pyrolytic Graphite by Scanning Tunneling and Atomic Force Microscopies

Samuel A. Hendricks,* Yeon-Taik Kim, and Allen J. Bard*

Department of Chemistry and Biochemistry, The University of Texas at Austin, Austin, Texas 78712

ABSTRACT

The electrodeposition and stripping of lead has been studied by *in situ* and *ex situ* scanning tunneling microscopy (STM) and *in situ* atomic force microscopy (AFM). The lead was electrodeposited on highly oriented pyrolytic graphite (HOPG). The HOPG was initially treated to produce monolayer deep pits which served as markers and supplied a high density of edge sites. Pb deposits preferentially formed at step and pit edges and resembled crystallite growth on a microelectrode disk. We discuss effects of tip potential on deposition during *in situ* STM and compare these results with AFM studies. After stripping, scanning microscopy and x-ray photoelectron spectroscopy indicated that residual Pb species remained on the surface.

We describe a study of the electrodeposition of Pb on highly oriented pyrolytic graphite (HOPG) by scanning tunneling microscopy (STM) and atomic force microscopy (AFM). Imaging of the surface in air after deposition and *in situ* study of the plating/stripping processes on HOPG under potential control are described. Pits on HOPG formed by air oxidation served in these studies as nucleation sites and markers. The STM has been used in a number of investigations in an electrochemical environment to study the electrode/solution interface.[1-5] Information on surface topography, as well as electronic structure, is available by this method. Although atomic resolution can be obtained with many substrates in air and vacuum,[6-8] the imaging of atomic structure for samples immersed in liquids is rare because of increased noise and drift.[3,9,10] However, the observation of features on the nm scale, *e.g.*, on single-crystal[11,12] and polycrystalline materials,[13,14] is also useful in the study of such processes as corrosion, polymerization, and thin film growth.

Several studies on the use of STM, and the related atomic force microscope (AFM), in electrodeposition investigations have appeared.[15-18] The bulk deposition of lead on HOPG was studied by Szklarczyk and Bockris[19] by STM. Observations of deposited lead from several to 100 monolayers in thickness by STM in air and in solution were claimed to reveal atomic images of the 111 and 100 crystal planes. The evolution of surface roughness was also observed upon dissolution of the Pb. A previous study on the deposition of Pb on HOPG is that of Morcos,[20] who reported underpotential deposition (UPD) of Pb, followed by deposition of the bulk metal. While other techniques such as electron microscopy,[21] field ion microscopy,[22] low energy electron diffraction (LEED), or reflection high energy electron diffraction (RHEED) can be used to study the early stages of metal electrodeposition, they are limited to *ex situ* application. This can cause changes in the surface structure upon removing the electrode from solution and placing in high vacuum. *In situ* electrochemical STM and AFM have a significant advantage over these other methods for electrochemical processes in allowing direct observation of the surface in the liquid. Moreover, *in situ* studies allow one to obtain images during different stages of the electrodeposition, and, if desired, stripping of the metal, as described below. However, it is useful in STM studies to monitor the deposition and stripping processes on the same area of substrate. Large differences are frequently observed when moving from one area of a surface to another, and one cannot be sure if electrochemical processes are responsible for the observed differences. Control of the substrate character is also an important factor in quickly finding an area suitable for study when experimental conditions are a function of time. A homogeneous surface, such as that found on HOPG, single-crystal gold, and layered materials, provides a uniform surface morphology for electrochemical studies. The production of monolayer pits by thermal treatment of HOPG was recently reported.[23] This pitted HOPG is very useful in Pb electrodeposition studies for several reasons. The patterns formed by the pits are unique from area to area, which gives an excellent network of landmarks that are easily and unambiguously identifiable. The use of pitted HOPG also allows one to study different reaction rates (*e.g.*, of deposition) at basal plane and edge sites.

Experimental

Samples of HOPG (generously provided by Dr. Arthur Moore, Union Carbide, Parma, OH) were prepared in the following manner. A clean surface was produced by cleaving the HOPG with a piece of sticky transparent tape. Next, the sample was heated in air for 5 min to a temperature of 650°C, cooled for 30 min, then heated in air again for 10 min. Substrates were inspected with the STM to verify the presence of etched pits. The depth of the pits on the HOPG samples measured from 3.5 to 7.5 Å in air and appeared deeper in solution. Based on previous STM investigations and STM and AFM studies of a number of HOPG samples, most of the observed pits were probably of monolayer depth (*i.e.*, 3.4 Å) and apparent variations are caused by differences in imaging conditions. The sample for *ex situ* imaging in air was prepared using a cell constructed of Teflon with a Viton O-ring, as shown in Fig. 1. Potential control was applied with a Princeton Applied Research (PAR) Model 173 potentiostat using a three-electrode configuration consisting of the HOPG working electrode, a platinum counterelectrode, and a saturated calomel reference electrode (SCE). The *ex situ* deposition of lead was carried out by sweeping the potential to −0.8 V and holding at this value until 2.8×10^{-3} C/cm^2 had passed. After the desired amount of charge was reached, the HOPG working electrode was disconnected, rinsed thoroughly with Milli-Q water (Millipore Corp., Bedford, MA), and dried prior to STM imaging.

In situ studies were carried out using the electrochemical cell provided with the Nanoscope II (Digital Instruments, Santa Barbara, CA). In this case the counterelectrode was a platinum wire and the reference was a silver wire. No difference in the electrochemical behavior was observed when lead was used as a reference electrode. Silver wire was used as a matter of convenience because of its availability in a suitable size and form. Tips were prepared by electrochemical etching of 250 μm diam 80:20 Pt/Ir wire (California Fine Wire, Grover City, CA) and coating them with Apiezon wax (Biddle Instruments, Blue Bell, PA) as described by Lindsay *et al.*[24] All images were obtained in the constant current (height) mode. The tip potential was

* Electrochemical Society Student Member.
** Electrochemical Society Life Member.

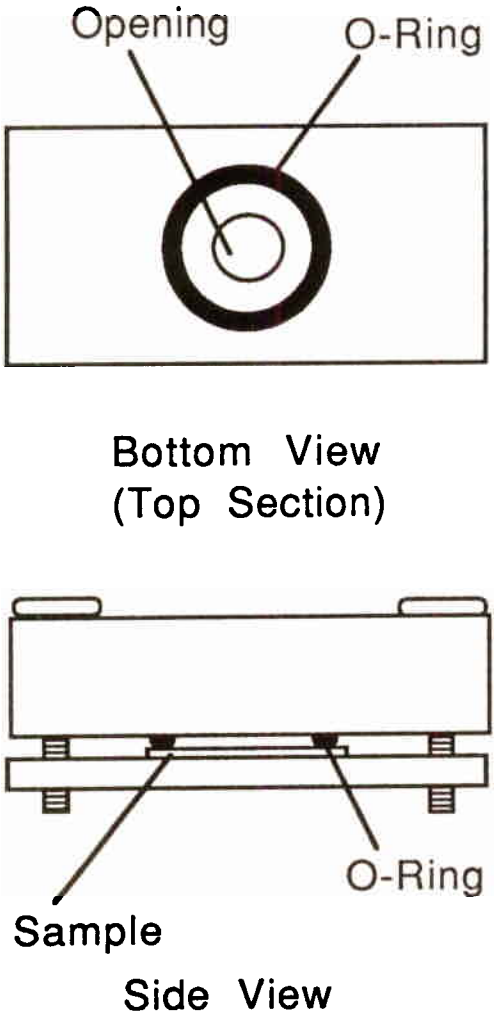

Fig. 1. Electrochemical cell used for sample preparation in *ex situ* studies. Diameter of exposed area is 3 mm and sample edges are shielded from solution.

held positive of the substrate in all cases to prevent deposition of Pb on the tip. The tip voltage *vs.* the reference electrode was initially adjusted to minimize faradaic current. Cyclic voltammetry was carried out to determine the deposition behavior of lead on HOPG. The substrate potential was then stepped between values where stripping and depositon occurred, while STM images as well as current plots were obtained.

All experiments, except for *in situ* AFM, were carried out in 0.5 m*M* $Pb(NO_3)_2$ solutions containing 1*M* $NaClO_4$ as supporting electrolyte. Solutions for *in situ* AFM were 1 m*M* in $Pb(NO_3)_2$. All solutions were prepared using Milli-Q water (18 mΩ-cm). XPS studies were carried out after stripping the lead to determine the residual lead species. X-ray photoelectron spectroscopic (XPS) analysis was performed with a VG ESCA Lab Mark I spectrometer (VG Scientific, Sussex, England) with a Mg x-ray source and an aluminum foil window. A beam current of 22 mA was employed for analysis. Operating pressure varied between 5×10^{-10} and 1×10^{-9} Torr. The constant analyzer energy (pass energy) was 20 eV with a spectrometer resolution of 1 eV. Samples were mounted using colloidal graphite paste on a stainless steel stub.

Results and Discussion

Cyclic voltammetry of Pb on HOPG.—Lead deposition was carried out on both thermally etched (pitted) and untreated freshly cleaved HOPG in 0.5 m*M* $Pb(NO_3)_2$/1*M* $NaClO_4$. As shown in Fig. 2, both samples showed a crossover of the cathodic current during the positive potential sweep. This phenomenon is well known[25] and occurs

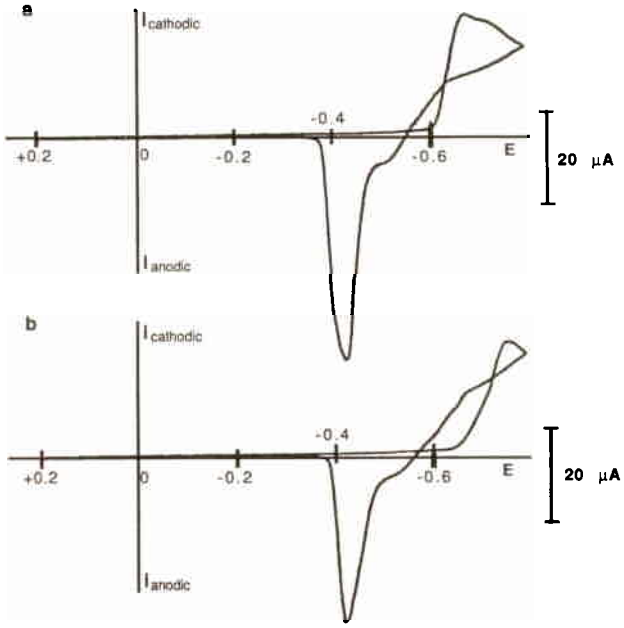

Fig. 2. Cyclic voltammograms at 50 mV/s of Pb deposition on (a) thermally etched highly oriented pyrolytic graphite (HOPG) and (b) freshly cleaved HOPG in 5×10^{-4} *M* $Pb(NO_3)_2$ and 1*M* $NaClO_4$.

when a nucleation overpotential is required to initiate deposition. The presence of metal nuclei increases the rate of Pb deposition permitting reduction to then occur at a more positive potential. With thermally etched HOPG (Fig. 2a), Pb deposition begins at about −0.60 V *vs.* SCE, while with freshly cleaved HOPG deposition begins at potentials about 40 mV more negative of this value. Thus the availability of a greater number of edge sites on pits on the HOPG surface appears to promote the formation of Pb nuclei. On the positive potential sweep, Pb deposition continues to a potential of about −0.57 V in both cases followed by an anodic peak for the stripping of Pb at −0.4 V.

Although underpotential deposition (UPD) of Pb on graphite was reported by Morcos[20] at 0.55 V positive of the potential for bulk Pb deposition, we did not find either a deposition or stripping peak in this potential region when using either a silver wire or lead reference electrode. All of our experiments indicate that Pb deposition of HOPG actually occurs with an overpotential. This overpotential arises from inhibited nucleation of Pb on the basal plane of HOPG. Nucleation at edge sites occurs at slightly less negative potentials (but still with an overpotential compared to bulk Pb deposition and stripping).

Ex situ STM studies of deposition.—After the passage of 2.8×10^{-3} C/cm^2, which corresponds to a coverage equivalent to *ca.* ten monolayers, the etched HOPG sample was disconnected, rinsed with water, and dried thoroughly by blowing nitrogen over the surface for about 5 min, until no visible evidence of solution remained, prior to imaging. Before Pb deposition, the STM images of the pitted HOPG showed only the roughly circular pits and channels (the latter ascribed to catalyzed HOPG air oxidation) as seen previously,[23] with no surface particles. After deposition (Fig. 3), clusters of Pb were present only at the pit and step edges, but not on the basal plane. Figure 3a shows these edge deposits over a 2 μm × 2 μm area; similar images were obtained at different locations on the substrate. A higher resolution scan (Fig. 3b) shows small Pb clusters (10-50 nm diam) on the pit edges. When deposition was carried out on nonpitted HOPG, no deposition was seen on the basal plane and Pb nuclei were found only at the step edges. The amount of lead deposited (equivalent to ten monolayers or a 35 Å thick layer), calculated from the charge passed, is much larger than the amount of lead seen by STM at the edge of the pits. This can be attributed to several causes. When the substrate is disconnected from the potentiostat

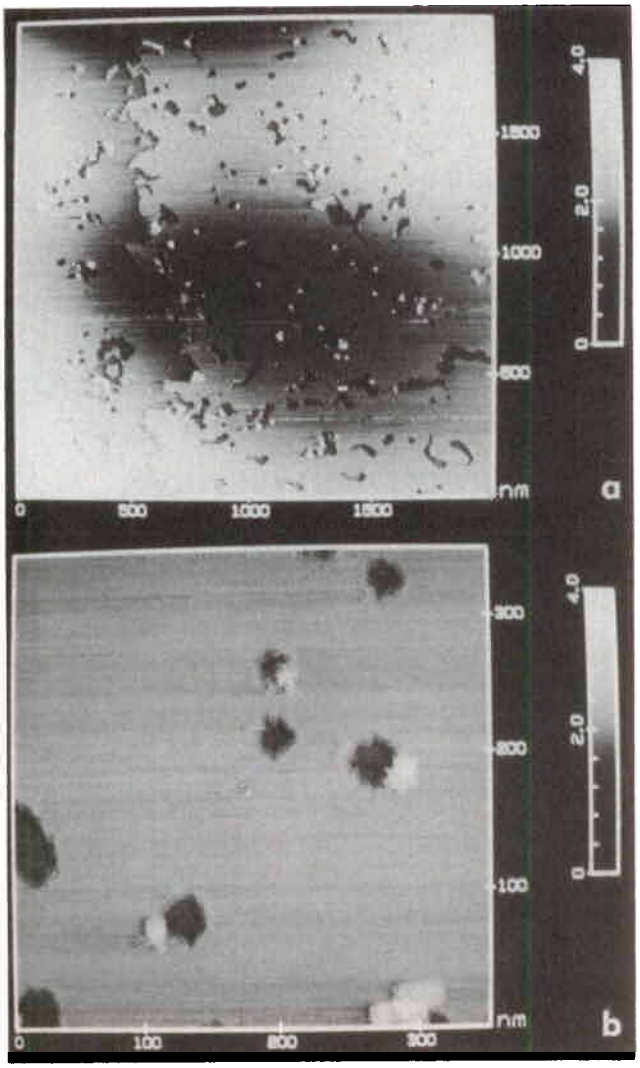

Fig. 3. *Ex situ* constant current STM images of Pb deposited on thermally etched HOPG from 0.5 m*M* $Pb(NO_3)_2$ in 1 *M* $NaClO_4$ showing particles distributed over (a) a 2000 nm × 2000 nm area and (b) a 350 nm × 350 nm area revealing more detailed particle structure. Tunneling bias, 327 mV; current, 0.51 nA.

and still in the deposition solution, some of the surface Pb is oxidized by oxygen in the solution. After removal from the solution, further oxidation of the Pb on the HOPG surface by oxygen in the rinse water or the air is also possible.

To study the factors affecting the stripping of deposited Pb from the HOPG surface, coulometric experiments, involving integration of the current under the cyclic voltammetric cathodic (deposition) and anodic (stripping) peaks, were carried out under different conditions. During a potential cycle from 0.0 to −1.1 V *vs.* AgQRE in a nondeaerated solution at v = 100 mV/s, the area under the anodic (stripping) peak was only 27% of that under the cathodic (deposition) peak. This ratio, R = 0.27, was independent of the anodic limit of the scan and was the same for scans to 1.0 V. Larger values of R were found when the solution was deaerated by bubbling Ar through it for 10 min before the voltammetric experiment and blanketing the solution with Ar during the scans. In this case R was 0.40 at 100 mV/s. Thus less Pb is lost from the surface in deaerated solutions, although significant differences in the amounts of current found for the anodic and cathodic still exist. The low values of R also suggest loss of Pb from the HOPG surface after deposition or reaction to form a nonoxidizable form. For example, the adhesion of the deposited Pb to the basal plane may be poor, so that Pb can become detached, especially during rinsing and removal of the HOPG sample following deposition. This would leave only the Pb at the pit edges, where it presumably is held more strongly. Thus *ex situ* studies suffer from problems of removal of the sample from the electrochemical cell and transfer to the STM environment.

In situ deposition (tip potential ≥ 0.7 V).—For *in situ* studies, samples were stepped to a potential of −1.00 V where cathodic current (≥ 40 μA/cm²) was passed, while the tip, held at a potential of +0.7 V, was scanned over a 650 × 650 nm portion of the surface. However, in most cases, passage of current for periods of up to 45 min revealed no topographic evidence of Pb deposition in the scanned area. Following these extended plating periods, the sample was removed and visual inspection revealed a dull film covering the entire substrate. *Ex situ* STM images obtained on more than ten areas of the surface indicated that the HOPG was totally covered with metal, *i.e.*, all areas of the surface were covered with Pb except that of the original scanning area. Thus, deposition is inhibited by the tip, which is held at a potential positive to the substrate. This can be explained by the presence of an electric field between tip and substrate which can affect potential distribution across the HOPG, making that in the area directly below the tip less negative than that for the rest of the surface, and insufficient for Pb deposition to occur. However, when current was passed for longer periods, we observed features suggesting that Pb moved into the viewing area from surrounding locations. Note that once nucleation occurs, Pb growth takes place at less negative potentials (see Fig. 2). Thus at a tip potential of +0.7 V and a substrate potential of −1.0 V, the substrate/electrolyte interfacial potential is apparently insufficiently negative to nucleate Pb deposition, but not sufficiently positive to strip existing Pb deposits. One such event is presented in Fig. 4, where Pb deposition and stripping at a single pit could be followed. Figure 4a shows Pb contained within a single pit after deposition by holding the substrate at −1.00 V for 45 min. Streaks in the image are attributed to mobile Pb which is pushed along the surface by the scanning tip. In spite of the noise, features can be seen to grow within the pit during deposition. A shift of the potential to −0.10 V, where anodic dissolution of lead is expected, caused removal of the lead (Fig. 4b). Subsequent deposition at −1.00 V on the same pit is shown in Fig. 4c-e. These show the formation of nuclei which grow with deposition time. Note that some deposition of Pb on areas of the basal plane surrounding the pit also can be seen in these figures. Note also that in Fig. 4b some Pb appears to remain following the stripping cycle. After growing Pb in the pit, the sample was returned to a potential of −0.10 V where the lead was again removed.

In situ deposition (lower tip potential).—As discussed above, a HOPG potential of −1.00 V, where reduction occurs, could be maintained for long periods of time (>45 min) before any deposition was observed under the tip (held at a potential above +0.70 V). When the tip was held at less positive potentials, *e.g.*, −0.40 V, but still in a region where Pb deposition was not possible, Pb deposition on the HOPG substrate beneath the tip could be observed. With this tip potential, the substrate was stepped to −0.60 V, which is at the foot of the bulk deposition peak, an immediate change in the surface was seen. Features suggesting Pb deposits became evident around the edges of the etched pits as shown in Fig. 5. Note that the material appearing at the edges of the HOPG pits seems to be concentrated more on the "downhill" side of the scan. That is, if the tip is moving from right to left, as is the case during data acquisition, the features appear on the left side of the pits. While most of the material is seen on the left side of the pits, there are still many features in other locations. Some of these are located on the right side of the pits. Note also that the features sometimes persist for several passes of the scanning tip. If poor tracking by the STM feedback system were the source of these features, this would indicate that the feedback circuit is making the same error on consecutive passes. Moreover, the features persisted at different scan rates. At slower scan rates there was no visible change in the images

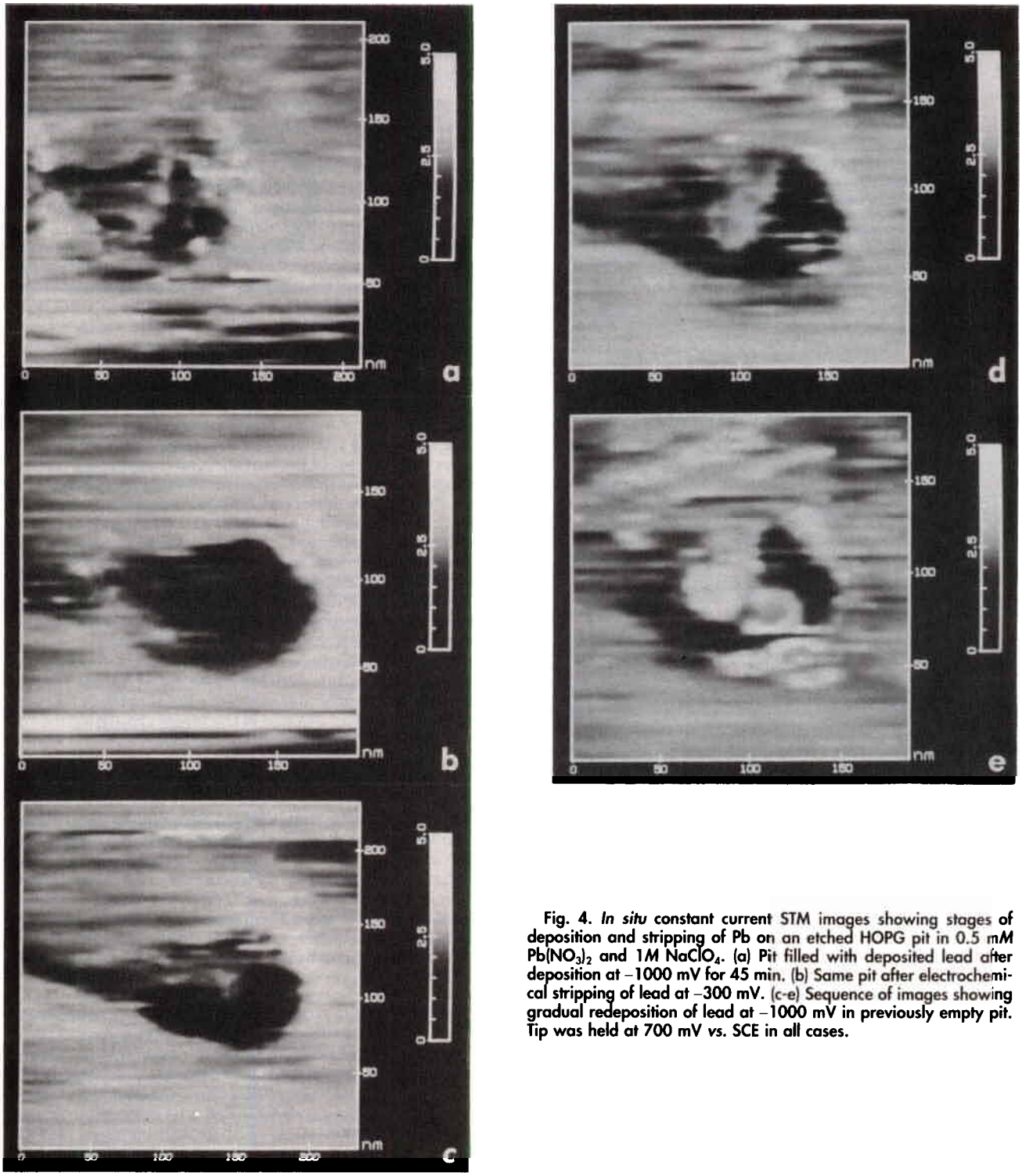

Fig. 4. *In situ* constant current STM images showing stages of deposition and stripping of Pb on an etched HOPG pit in 0.5 m*M* $Pb(NO_3)_2$ and 1 *M* $NaClO_4$. (a) Pit filled with deposited lead after deposition at −1000 mV for 45 min. (b) Same pit after electrochemical stripping of lead at −300 mV. (c-e) Sequence of images showing gradual redeposition of lead at −1000 mV in previously empty pit. Tip was held at 700 mV *vs.* SCE in all cases.

obtained. Slightly higher scan rates also yielded similar images. However, if the scan rate was increased drastically, the image quality deteriorated due to increased noise. A possible cause of the noise and the Pb location is the movement of Pb on the HOPG surface because of a strong interaction between the tip and metal particles, as has been reported in other cases.[26] The particles may find themselves pushed along the surface until contacting the pit edge where they are caught and the tip is allowed to pass over them. Streaks seen in Fig. 5 are probably also due to Pb which has been pushed over the pit edge and along the surface while imaging. The sequence of images along with substrate potential displayed in Fig. 6 on a single area of the substrate shows deposition, when the potential is stepped to a value where deposition occurs, followed by the stripping of lead when the HOPG is returned to the initial potential. These images also illustrate the advantages of the modified (pitted) HOPG surface. There is no question that the image location is the same in all three images. Moreover, the high density of monolayer steps produced by the pits shows that the observations are characteristic of pit and step edges rather than random behavior which can only be observed at selected sites. As previously mentioned, Pb can also be deposited on, and then stripped from, the edges of the pits by appropriate adjustment of the potential.

Pb morphology and XPS studies.—The morphology of lead deposited in each of the three cases discussed above was different. For the *ex situ* case, the observed features

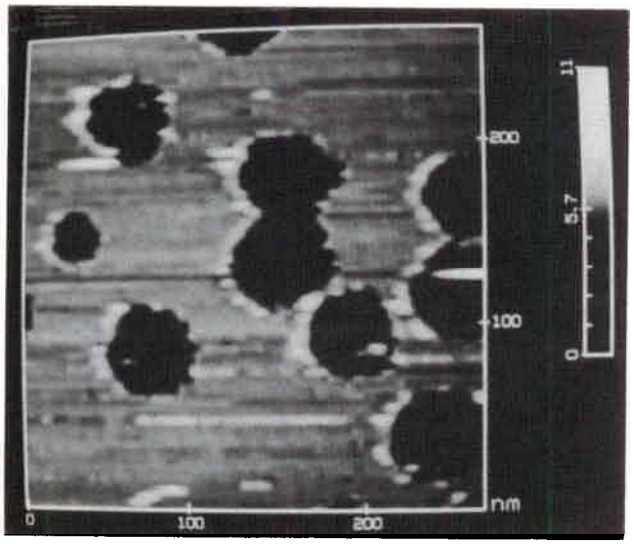

Fig. 5. *In situ* STM image of Pb located around edges of pits. Deposition was carried out at −600 mV *vs.* SCE with tip ramped from 382 to −400 mV and back in 0.5 m*M* $Pb(NO_3)_2$ and 1*M* $NaClO_4$. Imaging was done with tip at 382 mV *vs.* reference and a set point current of 5 nA.

are firmly attached to the surface. They are somewhat disk shaped and seem to be aggregated at or near the edge of the pits. The positive tip *in situ* experiments showed features which followed a nucleation and growth type of formation. In the negative tip *in situ* experiments, however, there is very poor definition of the particles, although they are undoubtedly present, with indications of mobility due to poor surface contact. Streaks across the surface also suggest the movement of the particles when in contact with the tip. This is consistent with the idea that Pb deposited on HOPG is not well anchored.

These three observations may be explained in the following way. For the *ex situ* case, the sample was allowed to dry thoroughly and during this period particles were able to diffuse and become anchored at the pit edges and to aggregate into larger particles with good electrical contact to the surface. The stability of these particles gives good definition to the images acquired.

In the first *in situ* case, the Pb grew in from the edge of the scanning area. Because discoloration was observed over the entire sample surface at this time, nucleation and growth of a bulk Pb phase occurs away from the tip and enters the scanning area by lateral growth. This lead can be

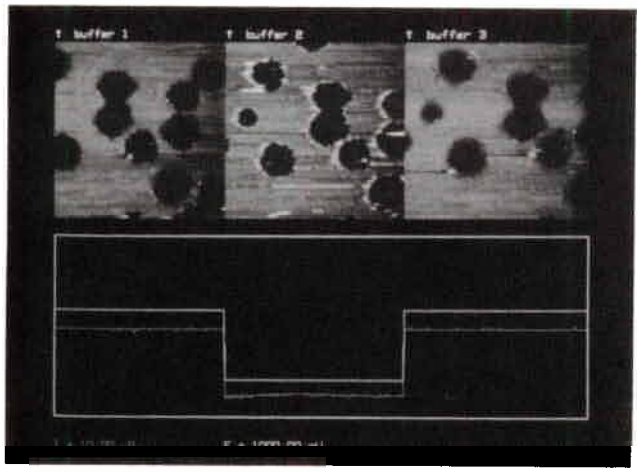

Fig. 6. Sequence of three *in situ* STM images with substrate potential showing the subsequent deposition and stripping on a single area of thermally etched HOPG. Deposition was carried out at −600 mV *vs.* SCE with the tip ramped from 382 to −400 mV and back in 0.5 m*M* $Pb(NO_3)_2$ and 1*M* $NaClO_4$.

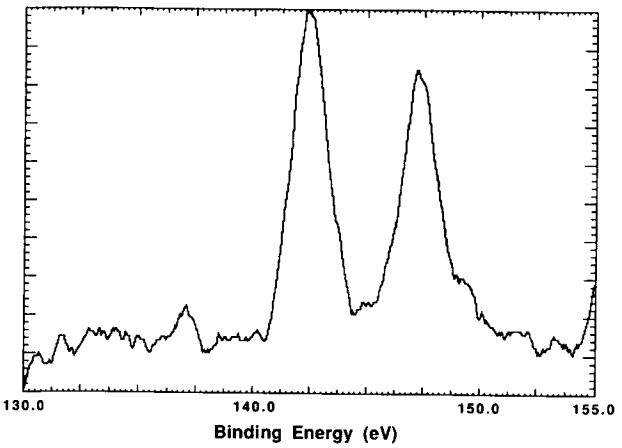

Fig. 7. X-ray photoelectron spectroscopy (XPS) of pitted highly oriented pyrolytic graphite (HOPG) after electrochemical deposition and stripping of Pb. Beam current, 22 mA; 20 eV pass energy; 1 eV spectrometer resolution. Operating pressure, 5×10^{-10} to 1×10^{-9} Torr.

imaged with reasonable definition in this case, because it is stabilized by being anchored to bulk phase outside of the scanning area. Upon stripping, all of the Pb is not removed. Evidence of this is seen in the XPS studies shown in Fig. 7, where Pb is detected on the HOPG surface after the HOPG was subjected to a potential where stripping should occur. Correction of the observed peaks based on the C 1s binding energy gives values of 139.3 and 144.5 eV corresponding to Pb 4f binding energies. Asymmetry, seen as small shoulders on the high-energy side of each peak, is due to an oxide form of the lead. Formation of this oxide may occur in solution, as discussed earlier, or upon exposure to air during transport of the samples from solution to the XPS chamber. Pb aggregates that remain behind are able to serve as nucleation sites for subsequent deposition. This is also supported by the increased density of deposition sites observed in later plate/strip cycles.

The second *in situ* experiment is somewhat harder to explain. For the *in situ* deposition below the tip, the freshly deposited lead adheres less strongly to the HOPG, because bulk Pb was not yet formed and tip interactions prevent detailed images of the smaller Pb deposits in most cases.

AFM studies.—In AFM studies, force is monitored instead of tunneling current and the tip (Si_3N_4) is an insulator and hence does not electrically affect the substrate. This enables the AFM to image nonconducting material or structures that do not make electrical contact with the substrate. AFM is particularly useful in electrochemical studies, since one need not be concerned about faradaic processes at the tip.[17] Moreover, the tip should perturb the electrical potential distribution on the substrate less in AFM than in STM.

Initial AFM studies of Pb deposition were done by controlling the substrate potential in an aqueous solution of $1.0 \times 10^{-3}M$ $Pb(NO_3)_2$ and 1.0*M* $NaClO_4$. With a three-electrode configuration with a silver wire quasi-reference (AgQRE), the potential of the substrate was first ramped to a value where deposition began (*ca.* −0.1 V *vs.* AgQRE). Prior to subjecting the substrate to the potential ramp, the HOPG sample was imaged and pits were routinely observed in electrolyte and at a potential of 0.0 V as shown in Fig. 8. The image in Fig. 8a demonstrates a typical pit density found on the heat-treated HOPG, while Fig. 8b is a cross-sectional area which indicates that the pit depth is of the order of one monolayer. While the measured depth of the pits varied somewhat and seemed to be dependent on factors such as tip condition and force, the lower limit of *ca.* 3.4 Å seen after many measurements probably reflects the actual depth in the absence of factors affecting the tip. Although the pits are clearly seen by AFM, the definition in these images is inferior to that obtained by STM. Brief ex-

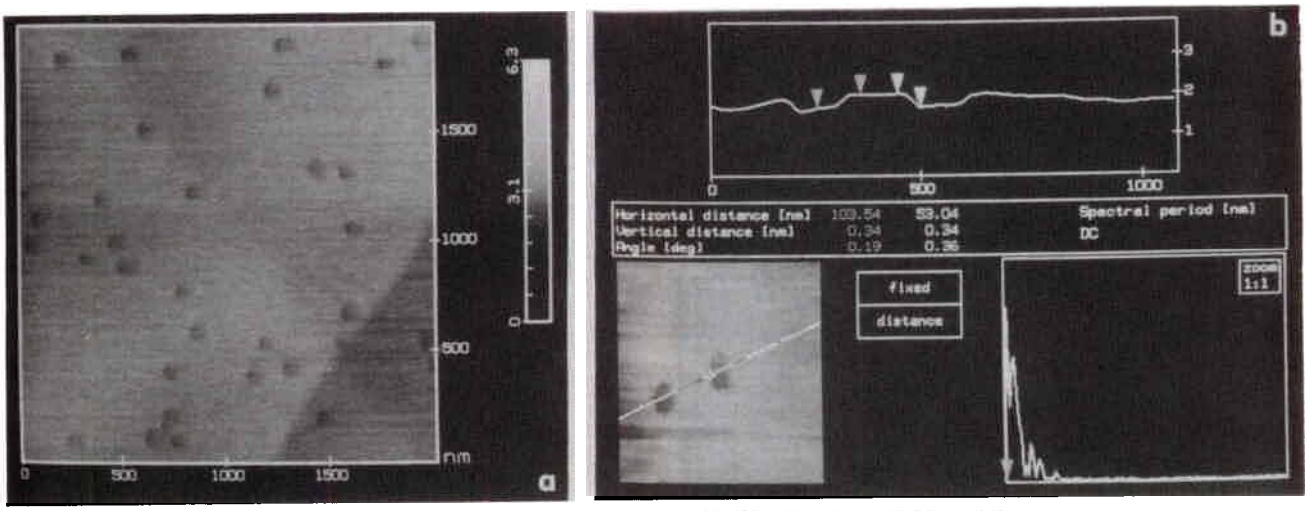

Fig. 8. (a) Atomic force microscope (AFM) image of 2 μm × 2 μm area on highly oriented pyrolytic graphite (HOPG) in aqueous solution of 1×10^{-3} *M* $Pb(NO_3)_2$ and 1 *M* $NaClO_4$ using a long thick cantilever. Potential of substrate is 0.0 V vs. AgQRE. (b) Cross section of two pits showing depth profile.

cursions of potential to more negative values did not produce observable effects on the HOPG image until the onset of lead deposition at about −0.1 V *vs.* AgQRE. The overpotential effect on nucleation and growth caused the deposition to proceed so rapidly at this point that images became noisy and pits were quickly covered and obscured. By greatly increasing the *z* range, sensitivity was lost but the deposition of relatively large amounts of Pb could be observed, as shown in Fig. 9. When the potential was swept in the positive direction, the features disappeared leaving the bare HOPG surface. This sequence could be repeated for a period of about 2 h before the images became noisy, possibly because of material picked up on the probe tip. Even at the lower resolution used to acquire images in Fig. 9, the Pb could be seen to accumulate at step edges rather than on the basal plane. Although the formation of islands was observed while scanning, these moved across the surface as the tip scanned. Larger islands were much more stable than small ones. When the tip was moved to another area of the surface, features initially seemed to be anchored more firmly and were more difficult to dislodge. This indicates that the Pb is somewhat mobile on the surface and is either formed on or is caught at pit and step edges where further growth can occur. Only a small volume of solution can be used in the AFM electrochemical cell, and Pb depletion from solution resulted in a drop in deposition current and was responsible for limiting the size of Pb islands. The islands themselves appear to be angular in shape suggesting a crystalline nature, although this observation may also be an artifact due to tip geometry.

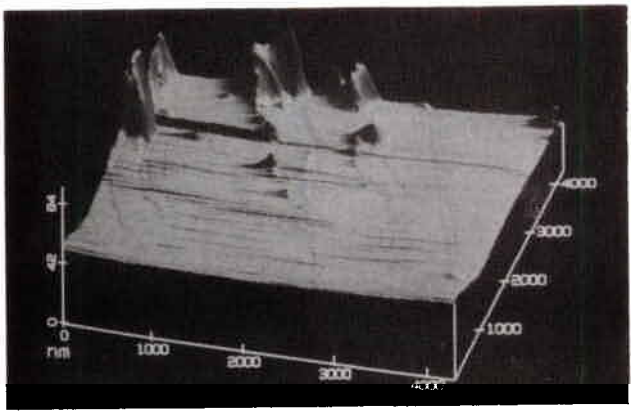

Fig. 9. Atomic force image of 4 μm × 4 μm area on HOPG in aqueous solution of 1×10^{-3} *M* $Pb(NO_3)_2$ and 1 *M* $NaClO_4$ with potential held at −0.1 V *vs.* AgQRE. *Z* range is 100 nm.

One of the goals of the experiment was to see if deposition occurred at step or pit edges. Although the Pb islands were discernible along step edges in the controlled potential experiments, the resolution was not sufficient to observe the initial stages of the deposition process. By performing the deposition of Pb galvanostatically, the rate of formation of Pb structures could be controlled and the sensitivity increased to the point where individual pits could be monitored during the early stages of nucleation. Although the voltage-time profile during controlled current experiments may differ from that using controlled potential, the amount of Pb deposited can be limited to amounts that allow high resolution images to be obtained.

The exposed surface area of the HOPG electrode was about 50 mm^2 and required the passage of *ca.* 2.8×10^{-4} C/cm^2 (*i.e.*, a 5 s pulse of 28.5 μA) to deposit 1 monolayer of Pb on the exposed area. The repeated application of this amount of current produced some very small features at the pit edges which disappeared after one or two scans indicating the formation of mobile nuclei at the edges which were swept away by the tip. After ten of these pulses, the current was increased to 200 $\mu A/cm^2$ and applied for 30 to 45 s until features appeared. In Fig. 10a, the Pb can be seen clearly at the pit and step edges. Application of additional current pulses, as in Fig. 10b, produced an increase in the amount of Pb deposited, along with the onset of instability of the images as seen earlier in controlled potential experiments. At the higher resolution obtained in the controlled current experiments, the instability appears to be caused, at least partially, by the existence of mobile Pb on the surface giving a streaked appearance to the images. When the scanning area was moved to other substrate areas, the amount of Pb present was greater as would be expected from the lack of physical interaction with the tip during the first stages of nucleation. The deposited Pb was easily removed as in previous experiments by a reversal of the current passed on the substrate. These experiments, combined with STM observations, provide strong evidence that Pb is deposited at edges in the early stages of deposition, with growth of nuclei at these sites until the surface is completely covered. The nucleation of Pb can occur directly under the AFM tip during scanning, as opposed to an STM tip held at a potential which can affect the substrate surface potential. While the nuclei formed are mobile on the surface, they adhere to the pit and step edges and are stabilized as their size increases.

Conclusions

Electrodeposition and stripping of Pb on an HOPG substrate that has been treated thermally to produce monolayer deep pits was studied by *ex situ* and *in situ* STM as well as *in situ* AFM. This allowed the direct observation of

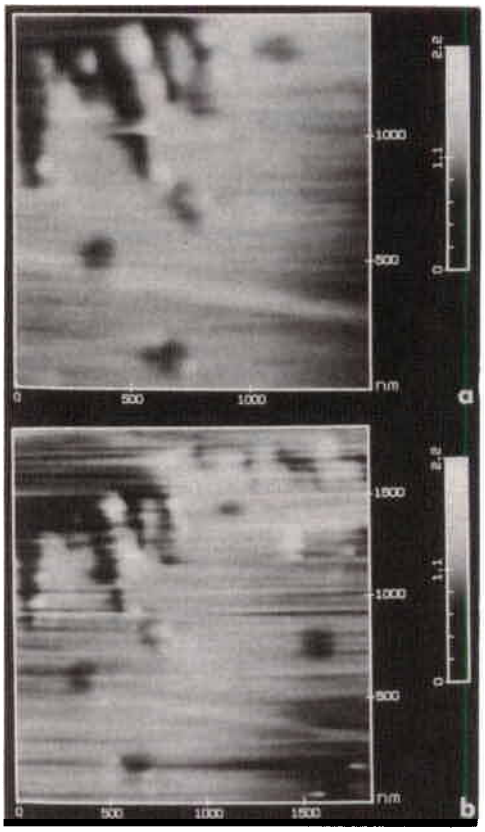

Fig. 10. (a) *In situ* AFM image of a 1.5 μm × 1.5 μm area on HOPG showing lead deposited at pit and step edges after a controlled current pulse of 100 μA for 45 s in an aqueous solution of 1×10^{-3} *M* $Pb(NO_3)_2$ and 1 *M* $NaClO_4$. (b) A 2 μm × 2 μm image of the area shown in part a after an additional 30 s pulse at 100 μA.

an area of interest during different stages of the deposition. The modification of the HOPG substrate allowed identification of a particular area and supplied a high density of edge sites. The direct observation of Pb deposition during initial stages of deposition showed that the metal is located primarily at edge sites and that growth is affected by interactions with the scanning probe tip. By varying the potential of the STM tip between −0.4 and 0.7 V *vs.* AgQRE we were able to observe a deposition dependence on the tip potential in the scanning area which we attributed, at least partially, to the alteration of the potential distribution on the substrate by the close proximity (<10 Å) of the biased tip and also to the interaction between the scanning probe and the reduced species. Additional studies by *in situ* AFM support these conclusions showing the formation of mobile Pb nuclei when an insulating tip is used. Stability of the Pb is increased with particle size. The images of deposited Pb suggest a crystalline morphology in both the STM and AFM studies, although the probe tip geometry is also important in AFM. XPS studies confirmed the existence of residual Pb after holding the substrate at a potential where the metal should be oxidized. Coulometric experiments also suggest that the reduced Pb is not completely stripped from the HOPG surface and is involved in some chemical process with oxygen.

Acknowledgments

The support of this research by a grant from the U.S. Office of Naval Research is gratefully acknowledged.

Manuscript submitted Feb. 10, 1992; revised manuscript received June 5, 1992.

REFERENCES

1. R. Sonnenfeld and P. K. Hansma, *Science,* **232,** 211 (1986).
2. H. Y. Liu, F.-R. Fan, C. W. Lin, and A. J. Bard, *J. Am. Chem. Soc.,* **108,** 3838 (1986).
3. R. Sonnenfeld and B. C. Schardt, *Appl. Phys. Lett.,* **49,** 1172 (1986).
4. B. Trake, R. Sonnenfeld, J. Schneir, and P. K. Hansma, *Surf. Sci.,* **181,** 92 (1987).
5. K. Itaya and S. Sugawara, *Chem. Lett.,* 1927 (1987).
6. G. Binning and H. Rohrer, *Helvetica Physica Acta,* **55,** 726 (1982).
7. J. A. Golouchenko, *Science,* **232,** 48 (1986).
8. R. Miranda, A. M. Baró, R. Garcia, J. L. Peña and H. Rohrer, *Appl. Phys. Lett.,* **47,** 367 (1985).
9. A. Gewirth and A. J. Bard, *J. Phys. Chem.,* **92,** 5563 (1988).
10. O. M. Magnussen, J. Hotlos, R. J. Nichols, D. M. Kolb, and R. J. Behm, *Phys. Rev. Lett.,* **64,** 24, 2929 (1990).
11. P. Lustenberger, H. Rohrer, R. Christoph, and H. Siegenthaler, *J. Electroanal. Chem.,* **243,** 225 (1988).
12. O. Lev, F.-R. Fan, and A. J. Bard, *This Journal,* **135,** 783 (1988).
13. J. Schneir, V. Elings, and P. K. Hansma, *ibid.,* **135,** 277 (1988).
14. F.-R. Fan and A. J. Bard, *Anal. Chem.,* **60,** 751 (1988).
15. R. S. Robinson, *J. Vac. Sci. Technol. A,* **8,** 511 (1990).
16. M. J. Armstrong and R. H. Muller, *This Journal,* **136,** 584 (1989).
17. S. Manne, P. K. Hansma, J. Massie, V. B. Elings, and A. A. Gewirth, *Science,* **251,** 183 (1991).
18. R. Sonnenfeld and B. C. Schardt, *Appl. Phys. Lett.,* **49,** 1172 (1986).
19. M. Szklarczyk and J. O'M. Bockris, *This Journal,* **137,** 452 (1990).
20. I. Morcos, *J. Electroanal. Chem.,* **66,** 250 (1975).
21. K. Takayanagi and K. Yagi, *Trans. Jpn. Inst. Met.,* **24,** 337 (1983).
22. H. W. Fink and G. Ehrlich, *Surf. Sci.,* **173,** 128 (1986).
23. H. Chang and A. J. Bard, *J. Am. Chem. Soc.,* **112,** 4598 (1990); **113,** 5588 (1991).
24. L. A. Nagahara, T. Thundat, and S. M. Lindsay, *Rev. Sci. Inst.,* **60,** 10, 3128 (1989).
25. S. Fletcher, C. S. Halliday, D. Gates, M. Westcott, T. L. Win, and G. Nelson, *J. Electroanal. Chem.,* **159,** 267 (1983).
26. M. Kuwabara, K. A. Smith, and D. R. Clarke, *J. Appl. Phys.,* **68,** 12, 6520 (1990).

Reprinted from JOURNAL OF THE ELECTROCHEMICAL SOCIETY
Vol. 139, No. 10, October 1992
Printed in U.S.A.